Research Article

Neural Network Based Retrieval of Atmospheric Temperature Profile Using AMSU-A Observations

R. K. Gangwar,[1] A. K. Mathur,[1] B. S. Gohil,[1] and Sujit Basu[2]

[1] *Geo-Physical Parameter Retrievals Division, Atmospheric and Oceanic Sciences Group (EPSA), Space Applications Centre (ISRO),*
 Ahmedabad, Gujarat 380015, India
[2] *Brahmprakash Scientist, Space Applications Centre (ISRO), Ahmedabad, Gujarat 380015, India*

Correspondence should be addressed to R. K. Gangwar; rgphybhu@gmail.com

The present study describes artificial neural network (ANN) based approach for the retrieval of atmospheric temperature profiles from AMSU-A microwave temperature sounder. The nonlinear relationship between the temperature profiles and satellite brightness temperatures dictates the use of ANN, which is inherently nonlinear in nature. Since latitudinal variation of temperature is dominant one in the Earth's atmosphere, separate network configurations have been established for different latitudinal belts, namely, tropics, mid-latitudes, and polar regions. Moreover, as surface emissivity in the microwave region of electromagnetic spectrum significantly influences the radiance (or equivalently the brightness temperature) at the satellite altitude, separate algorithms have been developed for land and ocean for training the networks. Temperature profiles from National Center for Environmental Prediction (NCEP) analysis and brightness temperature observations of AMSU-A onboard NOAA-19 for the year 2010 have been used for training of the networks. Further, the algorithm has been tested on the independent dataset comprising several months of 2012 AMSU-A observations. Finally, an error analysis has been performed by comparing retrieved profiles with collocated temperature profiles from NCEP. Errors in the tropical region are found to be less than those in the mid-latitude and polar regions. Also, in each region the errors over ocean are less than the corresponding ones over land.

1. Introduction

Numerical weather prediction (NWP) is crucially dependent on proper initialization of NWP models, which effectively boils down to an accurate estimation of the present atmospheric state, a vitally important component of which is the atmospheric temperature profile. Such profiles can be estimated from observations taken by satellite-borne sounders operating in the microwave region of electromagnetic spectrum. The Advanced Microwave Sounding Unit (AMSU) A on board the latest generation of the National Oceanic and Atmospheric Administration (NOAA) polar orbiting satellites measures the outgoing radiances from the atmosphere and the Earth surface. With channels in the oxygen absorption band, AMSU-A is designed to retrieve the atmospheric temperature from about 3 hPa (~45 km) down to the Earth's surface. The AMSU sounding unit operates on board the NOAA satellites since 1998. AMSU-A has

11 channels located close to the oxygen absorption lines below 60 GHz and four window channels at 23.8, 31.4, 50.3, and 89 GHz. The instrument has instantaneous fields of view of 3.3° and sample 30 Earth views. Therefore, the AMSU observation scan angle varies from −48° to +48° with the corresponding local zenith angle reaching 58° [1–3]. The channel characteristics are given in Table 1.

Retrieval of temperature profile from satellite observations is an inverse problem, being at the same time also a highly nonlinear and ill-posed one, the solution of which requires efficient techniques. In the past, several retrieval techniques have been used. A very old technique is multiple linear regression, which is still used as a benchmark for judging the power of more modern techniques (e.g., [4]). An iterated minimum-variance based algorithm [5] was proposed earlier, while more recently 1-D variational method has been proposed by Boukabara et al. [6] for the retrieval of temperature profiles from AMSU-A observations.

TABLE 1: AMSU-A channel's specifications.

Channel number	Frequency (GHz)	Bandwidth (MHz)	Noise equivalent (K)
1	23.8	251.02	0.20
2	31.4	161.20	0.27
3	50.3	161.14	0.22
4	52.8	380.52	0.15
5	53.596 ± 0.155	168.20	0.15
6	54.4	380.54	0.13
7	54.94	380.56	0.14
8	55.5	310.34	0.14
9	57.290	310.42	0.20
10	57.290 ± 0.217	76.58	0.22
11	$57.290 \pm 0.322 \pm 0.0480$	35.11	0.24
12	$57.290 \pm 0.322 \pm 0.0220$	15.29	0.35
13	$57.290 \pm 0.322 \pm 0.0100$	7.93	0.47
14	$57.290 \pm 0.322 \pm 0.0045$	2.94	0.78
15	89.0	1998.98	0.11

Back propagation neural networks have also been used for the retrieval of atmospheric temperature profile from Advanced Microwave Sounding Unit-A (AMSU-A) measurements [4, 7]. This is because of their ability to efficiently handle inherently nonlinear problems. Other examples of neural network technique for the retrieval of atmospheric temperatures using IASI instrument and hyperspectral Fourier transform infrared dataset, respectively, are available in [8, 9]. Blackwell [10] very recently did an analysis of high-resolution profiling of atmosphere by considering hypothetical 87 channels microwave sounder using neural network. Also, Tao et al. [11] performed error variance estimation in retrievals of geophysical parameters using neural network technique.

Since the performance of these techniques depends on the dataset used for training the algorithm, the training dataset should faithfully represent the variabilities of the real atmosphere. The present study proposes an Artificial Neural Network (ANN) based approach for retrieving the atmospheric temperature profile. The structure of the paper is as follows. In the next section we describe the data and methodology including the explanation of ANN architecture used by us. This is followed by description of results and discussion in Section 3. The conclusions are presented in Section 4.

2. Data and Methods

We describe below the dataset used by us in the Section 2.1 followed by the methodology in Section 2.2 and a description about ANN in Section 2.3.

2.1. Data. Temperature profiles from NCEP GDAS analysis along with concurrent AMSU-A L1-B brightness temperature observations for the year 2010 have been used to establish the neural network configurations. The NCEP implemented operationally a series of numerical models for the generation of global model analyses and forecasts. One of the operational systems is Global Data Assimilation System (GDAS). The details of GDAS are available in Kalnay et al. [12]. Model output at analysis time and a 6-hour forecast are available from the National Oceanic and Atmospheric Administration (NOAA) National Operational Model Archive & Distribution System (NOMADS; http://nomads.ncdc.noaa.gov/) server.

Observations of all 15 channels of AMSU-A have been used. It is well known that each AMSU channel is extremely sensitive to temperature of a particular atmospheric layer starting from the troposphere and going right up to the lower stratosphere. Temperature profiles from NCEP have been taken at 26 pressure levels given in Table 2. AMSU-A has 48 km spatial resolution at nadir. NCEP temperature profiles of 1° spatial resolution at four synoptic hours, namely, 0000, 0600, 1200, and 1800 UTC, have been used. The data for 2010 have been used for developing as well as validating the retrieval algorithm. Moreover, a few months of data from the same two sources in 2012 have been used for further independent testing.

2.2. Methodology. We want to clarify at the outset that the entire study is for retrieval of temperature profiles in the clear-sky region. For delineating clear-sky region the following has been done. We have used simulation based threshold values of brightness temperatures for each channel of AMSU-A. The simulations were carried out for clear sky condition using diverse atmospheric profiles through RTTOV radiative transfer model. To exclude cloudy pixels from AMSU-A observations we have chosen only those pixels for which the brightness temperature of each channel is greater than the corresponding precomputed threshold. To develop the retrieval algorithm a training dataset has been created for tuning the neural network from the NCEP analysis as well as AMSU-A for the year 2010. A part of the data is for training the algorithm and the remaining part is withheld for validation. Due to different emission signatures of land and ocean at these microwave frequencies the neural network configurations have been established separately for land and ocean. Also the study area has been further subdivided into tropical, mid-latitude, and polar regions, respectively. This division into three separate regions is for the simple reason that the temperature profiles display quite different degree of variability in these regions as seen in Table 2. The variability is low in the tropics (30°S–30°N) and much higher in the polar regions ((90°S–60°S) and (60°N–90°N)). In the mid-latitude ((60°S–30°S) and (30°N–60°N)), it is in the intermediate range. Our aim is to derive temperature at specific pressure levels. Accordingly, for a particular region, neural networks are established separately for each pressure level. Once the retrieval at each level is done, with a specific network configuration, we combine the retrieved temperature at each level into a temperature profile.

AMSU-A observations have been resampled at NCEP grid resolution for spatial collocation. As far as temporal collocation is concerned, a time window of ±1 hr has been chosen. From the total number of collocated pairs in the

TABLE 2: Statistics of temperature fields from NCEP of the training dataset.

Pressure (hPa)	Tropical		Mid-latitude		Polar	
	Mean (K)	Standard deviation (K)	Mean (K)	Standard deviation (K)	Mean (K)	Standard deviation (K)
1000	299.75	5.59	288.70	11.23	263.50	12.44
975	297.48	5.64	282.32	11.15	262.69	12.17
950	296.10	5.58	280.96	11.06	262.09	11.87
925	294.76	5.42	279.66	10.91	261.46	11.59
900	293.48	5.16	278.46	10.72	260.79	11.40
850	290.09	4.45	276.20	10.28	259.29	11.20
800	287.85	3.60	273.93	9.84	257.50	11.10
750	285.64	3.09	271.41	9.51	255.42	10.99
700	281.64	2.73	268.57	9.30	258.08	10.72
650	279.13	2.57	265.40	9.12	250.70	10.07
600	275.77	2.57	261.74	8.99	247.98	8.96
550	271.42	2.62	257.66	8.90	244.61	8.16
500	267.30	2.74	253.01	8.84	240.34	7.92
450	262.51	2.93	247.74	8.74	235.46	7.66
400	256.05	3.14	241.74	8.54	230.00	7.26
350	249.48	3.17	235.11	8.09	224.14	6.68
300	241.29	3.04	228.14	7.18	218.82	6.22
250	231.68	2.60	221.94	6.08	216.53	7.78
200	220.35	1.96	218.67	5.89	217.37	10.00
150	207.49	2.42	217.04	5.52	217.18	10.69
100	195.66	4.46	214.31	6.59	215.86	11.89
70	199.45	4.44	214.22	6.09	215.09	13.01
50	206.94	3.51	215.52	5.23	214.76	13.95
30	215.67	2.72	218.18	5.68	215.41	15.22
20	222.01	2.66	221.04	6.82	217.16	16.13
10	230.22	3.23	227.19	8.98	223.02	17.21

year 2010 roughly 60% have been randomly chosen for training the algorithm, while the rest are used for validation. Similar collocation has been done in some months of 2012 for an independent testing of the algorithm. The collocation statistics is provided in Table 3. After the temperatures are retrieved, we have compared the retrieved profiles with collocated NCEP profiles and the strength of the algorithm has been quantified statistically in terms of BIAS and standard deviation (STD) of the difference.

2.3. Artificial Neural Network. Neural networks are composed of simple elements operating in parallel. The entire network design is inspired by biological nervous system. Hence the elements are called neurons. Typically, the neural networks are adjusted, or trained, such that a particular input pattern leads to a specific target output pattern. This is done by iteratively adjusting the weights interlinking the neurons. These networks have been trained to perform complex functions in various fields such as pattern recognition [13] and voice [14] and speech recognition [15]. There can be more than one layer in a neural network in which neurons of one

layer are interconnected with neurons of the other layers. A schematic of the neural network architecture used in this study has been shown in Figure 1. These layers are known as input, hidden, and output layers. Each layer has one weight matrix, a BIAS vector, and anoutput vector. There are three distinct functional operations, which take place in any neural network. First, the vector input $\mathbf{p}$ is multiplied by scalar weight $\mathbf{w}$ to form the product $\mathbf{wp}$. Second, this weighted input is added to a vector BIAS $\mathbf{b}$ to form the net input $\mathbf{n}$. Finally, the net input $\mathbf{n}$ is passed through a transfer function $\mathbf{f}$, which produces a vector output $\mathbf{a}$. Here, both $\mathbf{b}$ and $\mathbf{w}$ are adjustable parameters. By adjusting these parameters, one can achieve the desired training of the neural network.

The network should be chosen such that it could be able to model the nonlinearity of the problem. The most popular type of neural network and the one employed in our study is the feed forward back propagation neural network. A description about back propagation theory, its architecture, and its applications can be found in many publications, for example, [16–20]. In the present study, we have used feed forward back-propagation neural network with two hidden layers with 10 neurons in each hidden layer. The Input layer

TABLE 3: Number of collocated points used for estimating the temperature profiles.

	Tropical		Mid-latitude		Polar	
	Land	Ocean	Land	Ocean	Land	Ocean
Training (2010)	125179	165978	142027	156002	131799	155102
Validation (2010)	83453	110652	94686	104002	87867	103404
Testing (2012)	1902786	2670948	1305113	3288203	1845789	2314500
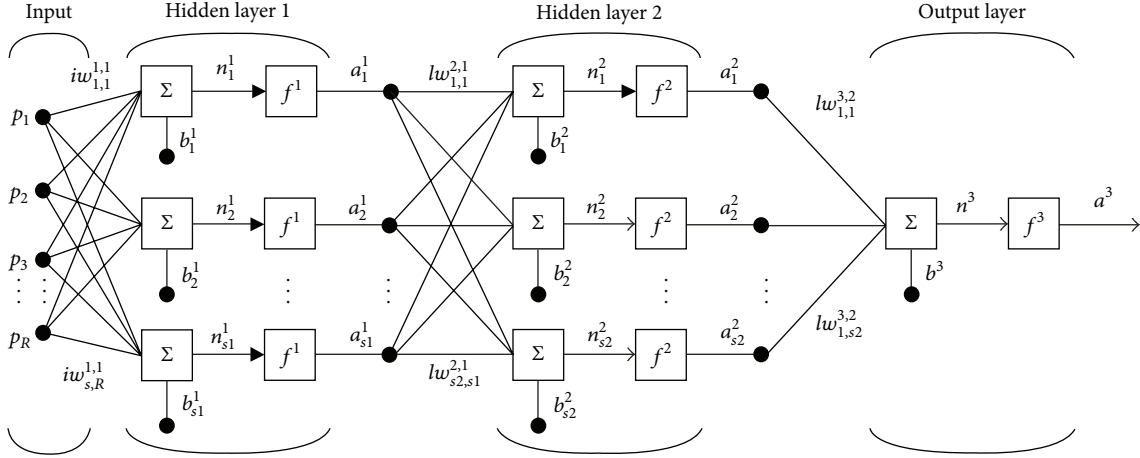
FIGURE 1: Schematic for three-layer neural network used for training.

has 16 elements, out of which 15 are the AMSU-A channel brightness temperatures and the remaining one is the satellite zenith angle. Temperature at a specific pressure level is the output of the neural network. The number of input neurons is fixed in each case for obvious reason. The output consists of only neuron. The numbers of hidden layers and the number of neurons in these layers are basically tuning parameters of the retrieval algorithm. We have kept these fixed at 2 and 10, respectively, for each retrieval. These optimum numbers have been determined by keeping on changing the numbers until one gets the optimum network performance. The transfer function used is Log-sigmoid in the first hidden layer and hyperbolic tangent sigmoid in the second hidden layer.

3. Results and Discussion

The retrieval algorithm explained above has been tested during four months (January, April, July, and November, 2012) of data. Since the algorithm has been developed for three geographical regions, the comparison has also been done accordingly. The month-wise statistics have been shown in Figures 2, 3, and 4 for these geographical regions separately. For a comprehensive picture, we have combined the errors for all the months for the individual geographical regions and these are shown in Figures 5–7.

Figure 5 shows the STD and BIAS for tropical regions. Over ocean the error lies between 1 K and 2 K for all the levels. Over land in lower troposphere, it is 3 K at 1000 hPa and decreases to around 2 K while it remains near to 1 K in mid-troposphere. A slightly higher error at tropopause has been found over both the surfaces.

Figure 6 shows the BIAS and standard deviation for mid-latitude regions over both land and ocean surfaces. From these figures it can be seen that over land in lower troposphere the STD is around 4 K at 1000 hPa and it then decreases to 2 K at 800 hPa, while over ocean from 1000 to 800 hPa STD is near to 2 K. The error is <1.5 K and <2 K in mid-troposphere over ocean and land, respectively. Except near tropopause the errors are around 1 K for upper troposphere as well as for lower stratosphere. The BIAS is between 0 and 0.5 K at each level except at one or two isolated levels. The higher errors over land can be attributed to higher emissivity and greater variations in surface characteristics.

The statistics for polar regions for land and ocean are shown in Figure 7. From this figure we can see that in the lower troposphere the STD is around 4 K at 1000 hPa and it then decreases to 2 K at 600 hPa over land surface, while the decrease is from 3 K to 1.5 K over ocean surface. For mid-tropospheric regions the error is near 1.5 K while, in the upper troposphere as well as in the lower stratosphere, errors are less than 1 K for both the surfaces.

It is worthwhile to investigate the reason for the higher errors in mid-latitude and polar regions compared to those in the tropics. Every instrument is designed for the measurement of a parameter for a specified range. If the variability of the parameter is higher than the specified range, the instrument may not be able to capture the actual variability, due to which a large error will occur in the measurement of the parameter. In the tropics the atmosphere is highly moisture-laden. The moisture absorbs the outgoing long wave radiation emitted by the earth. This absorption gives rise to the observed temperature structure in the tropics with
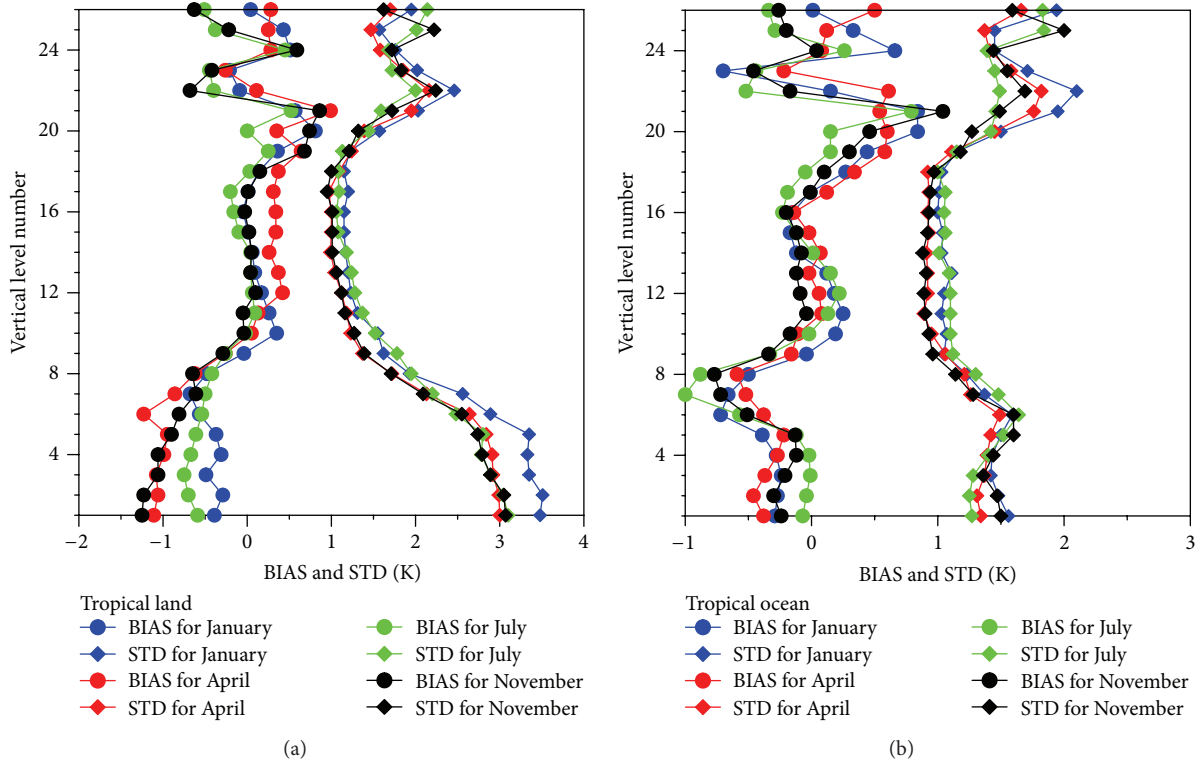
FIGURE 2: STD and BIAS for retrieved temperature profiles for tropical regions for different months over (a) land and (b) ocean.
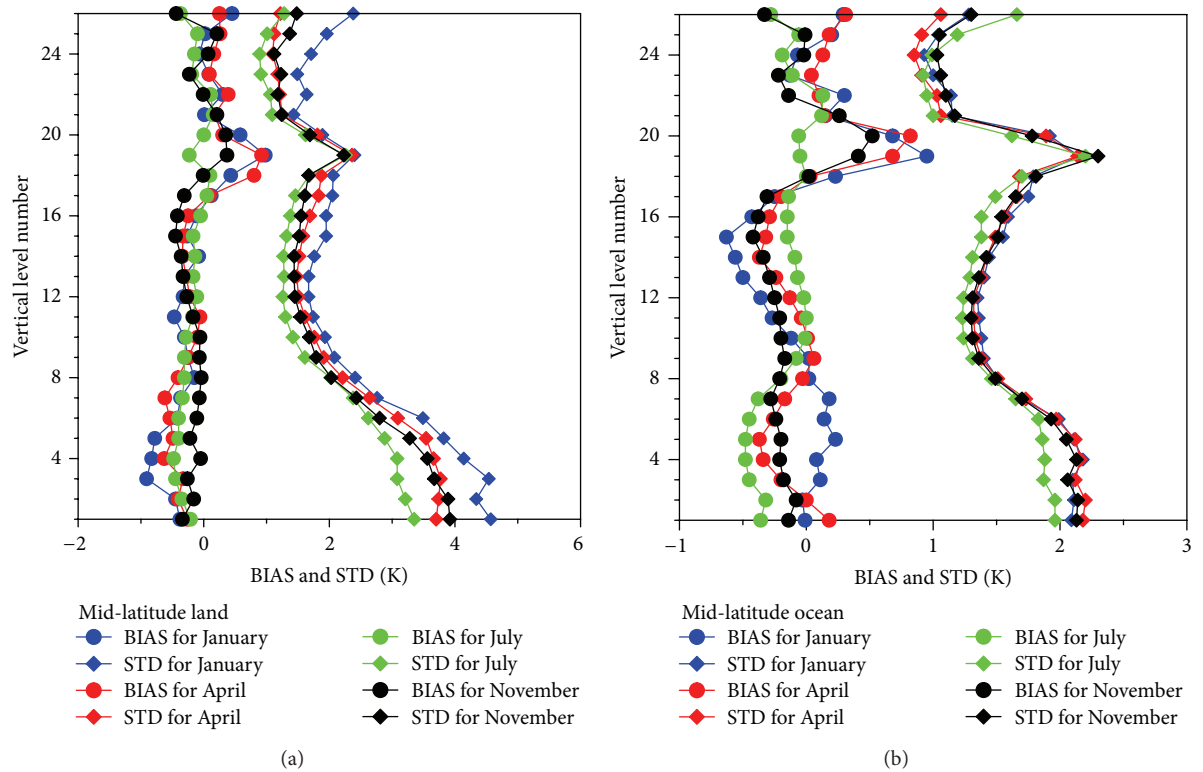

FIGURE 3: STD and BIAS for retrieved temperature profiles for mid-latitude regions for different months over (a) land and (b) ocean.
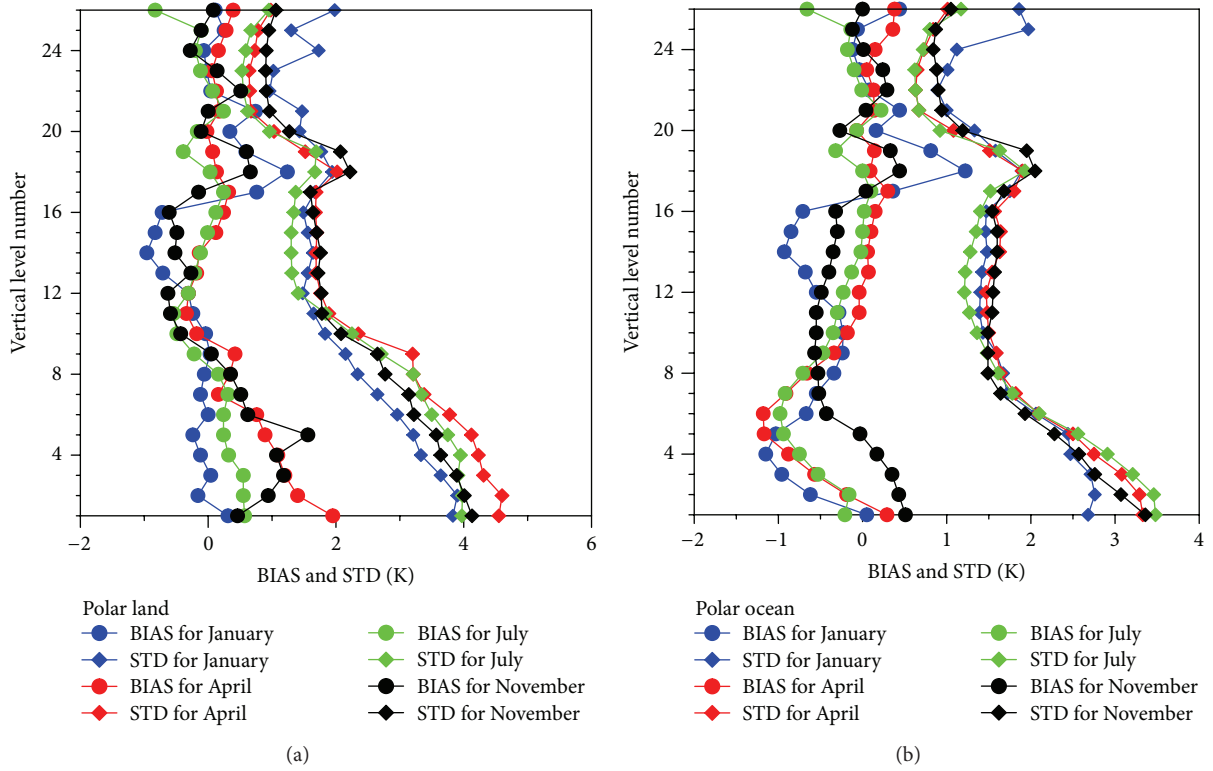
(a)

(b)

FIGURE 4: STD and BIAS for retrieved temperature profiles for polar regions for different months over (a) land and (b) ocean.
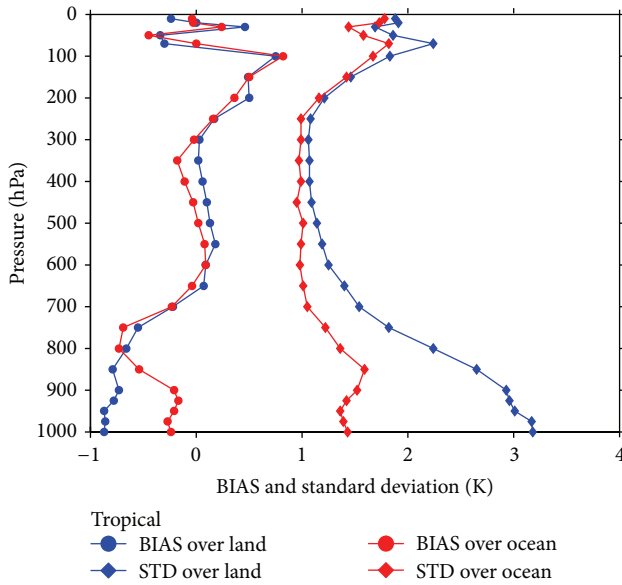

FIGURE 5: STD and BIAS for retrieved temperature profiles for tropical regions over land and ocean.
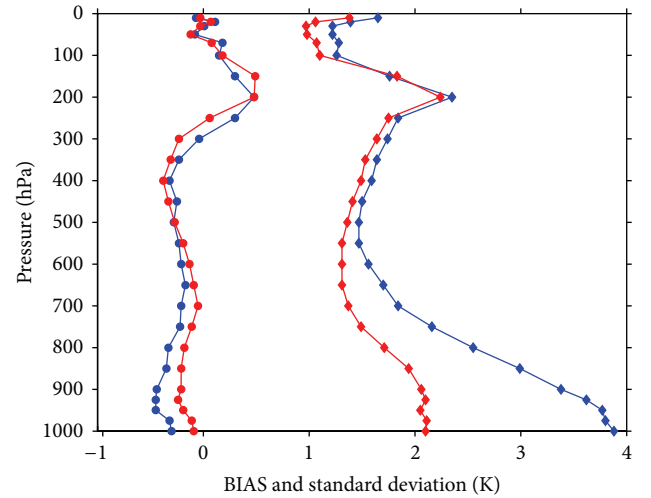

FIGURE 6: STD and BIAS for retrieved temperature profiles for mid-latitude regions over land and ocean.

moderate variability. On the other hand, in the mid-latitude and polar regions the atmosphere is generally dry (with low moisture) and the absorption due to moisture is absent. Consequently the temperature structure in these two regions is different from the tropics, with high variability. Because of

this high variability as seen from Table 2, the accuracies of retrieval are obviously less than the accuracy in the tropics.

It is also interesting to view our result in the perspective of the result of a similar study by Shi [4]. One difficulty is that Shi [4] is concerned with only over land. Since we have carried
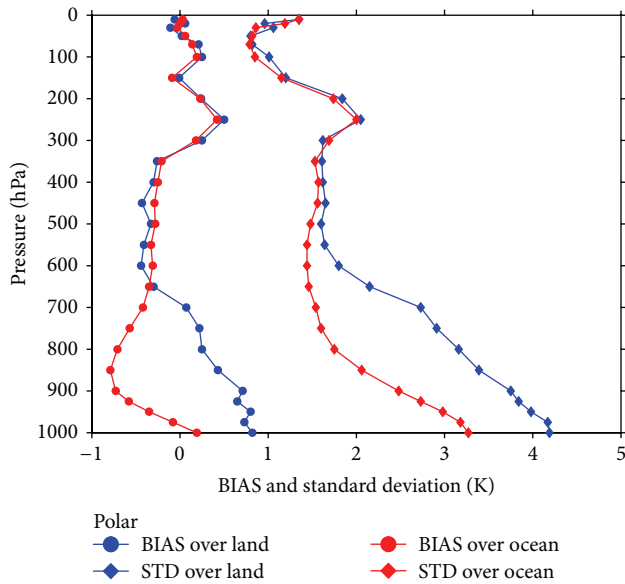
FIGURE 7: STD and BIAS for retrieved temperature profiles for polar regions over land and ocean.

out retrieval over ocean as well, a rigorous comparison is not possible. However, we can compare the corresponding errors over land. In Shi [4] study the root-mean-square deviation of temperature retrieval is 3.28 K at the surface, 1.08 to 1.28 K in the mid-troposphere, less than 1.58 K around the tropopause, and between 1.08 and 1.58 K in the stratosphere. In our study the retrieval error for land is about 3.5 K in the lower troposphere, is almost 1.5 K throughout the mid-troposphere, is about 1 K near tropopause, and is between 1.5 K and 2 K in the lower stratosphere. As regards oceans, we could not find a similar study involving ANN. However, in a recent study Boukabara et al. [6] retrieved the temperature profile over land and ocean surface separately using 1-d variational method. In their study they have provided errors with respect to GDAS analysis at five different pressure levels, namely 950, 800, 500, 300, and 100 hPa, over oceans. The standard deviation of the difference of the retrieved and model temperatures at these five pressure levels is 2.8, 1.7, 1.4, 1.6, and 1.5 K, respectively. In our study we have retrieved temperature profile for three geographical regions separately. In order to compare with Boukabara et al. [6], we combined the errors for all the three regions over oceans. At the designated pressure levels, the combined errors are 2.1, 1.6, 1.3, 1.4, and 1.2 K, respectively.

4. Conclusions

In this study we have exploited the capability of neural network for solving the nonlinear inverse problem of the retrieval of atmospheric temperatures profiles from satellite observations with reasonable success. Due to diverse nature of temperatures in different latitudinal zones, separate network configurations have been employed for three distinct latitudinal zones. The vertical profiles of retrieval errors are

shown in figures for each region and separately for land and ocean. There is a general tendency for the errors to be less in the tropical regions. A possible reason could be the higher temperature variability in the other two regions, namely, the mid-latitude and polar regions, which the sensors could not correctly capture. It can be said in the general terms that the results are comparable with past studies of similar natures. In future we will try to improve the algorithms by making the distinction between land and ocean clearer using more accurate microwave emissivity models. Also, we will try to distinguish between clear-sky and cloudy sky brightness temperatures using comprehensive radiative transfer models in the cloudy atmosphere.

Conflict of Interests

The authors declare that there is no conflict of interests regarding the publication of this paper.

Acknowledgments

References

[1] T. Mo, "Prelaunch calibration of the advanced microwave sounding unit—a for NOAA-K," *IEEE Transactions on Microwave Theory and Techniques*, vol. 44, no. 8, pp. 1460–1469, 1996.

[2] T. Mo, "AMSU-a antenna pattern corrections," *IEEE Transactions on Geoscience and Remote Sensing*, vol. 37, no. 1, pp. 103–112, 1999.

[3] G. Goodrum, K. B. Kidwell, and W. Winston, *NOAA KLM User's Guide*, National Oceanic and Atmospheric Administration, 1999.

[4] L. Shi, "Retrieval of atmospheric temperature profiles from AMSU-A measurement using a neural network approach," *Journal of Atmospheric and Oceanic Technology*, vol. 18, no. 3, pp. 340–347, 2001.

[5] P. W. Rosenkranz, "Retrieval of temperature and moisture profiles from AMSU-A and AMSU-B measurements," *IEEE Transactions on Geoscience and Remote Sensing*, vol. 39, no. 11, pp. 2429–2435, 2001.

[6] S.-A. Boukabara, K. Garrett, W. Chen et al., "MiRS: an all-weather 1DVAR satellite data assimilation and retrieval system," *IEEE Transactions on Geoscience and Remote Sensing*, vol. 49, no. 9, pp. 3249–3272, 2011.

[7] Z. Yao, H. Chen, and L. Lin, "Retrieving atmospheric temperature profiles from AMSU-A data with neural networks," *Advances in Atmospheric Sciences*, vol. 22, no. 4, pp. 606–616, 2005.

[8] F. Aires, A. Chédin, N. A. Scott, and W. B. Rossow, "A regularized neural net approach for retrieval of atmospheric and surface temperatures with the IASI instrument," *Journal of Applied Meteorology*, vol. 41, no. 2, pp. 144–159, 2002.

 [9] J. Cheng, Q. Xiao, X. Li, Q. Liu, Y. Du, and A. Nie, "Multi-layer perceptron neural network based algorithm for simultaneous retrieving temperature and emissivity from hyperspectral FTIR dataset," in *Proceedings of the IEEE International Geoscience and Remote Sensing Symposium (IGARSS '07)*, pp. 4383–4385, June 2007.

[10] W. J. Blackwell, "Neural network Jacobian analysis for high-resolution profiling of the atmosphere," *Eurasip Journal on Advances in Signal Processing*, vol. 2012, no. 1, article 71, 2012.

[11] Z. Tao, W. J. Blackwell, and D. H. Staelin, "Error variance estimation for individual geophysical parameter retrievals," *IEEE Transactions on Geoscience and Remote Sensing*, vol. 51, no. 3, pp. 1718–1727, 2013.

[12] E. Kalnay, M. Kanamitsu, R. Kistler et al., "The NCEP/NCAR 40-year reanalysis project," *Bulletin of the American Meteorological Society*, vol. 77, no. 3, pp. 437–471, 1996.

[13] G. L. Martin and J. A. Pittman, "Recognizing hand-printed letters and digits using backpropagation learning," *Neural Computation*, vol. 3, no. 2, pp. 258–267, 1991.

[14] M. A. Al-Alaoui, L. Al-Kanj, J. Azar, and E. Yaacoub, "Speech recognition using artificial neural networks and hidden Markov models," *IEEE Multidisciplinary Engineering Education Magazine*, vol. 3, no. 3, pp. 77–86, 2008.

[15] G. K. Venayagamoorthy, V. Moonasar, and K. Sandrasegaran, *Voice Recognition Using Neural Networks*, IEEE, 1998.

[16] J. E. Dayhoff, *Neural Network Architectures—An Introduction*, Van Nostrand Reinhold, 1990.

[17] J. Hertz, A. Krogh, and R. G. Palmer, *Introduction to the Theory of Neural Computation*, Addison-Wesley, 1991.

[18] A. Cichocki and R. Unbehauen, *Neural Networks for Optimization and Signal Processing*, John Wiley & Sons, 1993.

[19] Y. Chauvin and D. E. Rumelhart, *Backpropagation: Theory, Architectures, and Applications*, Lawrence Erlbaum Associates, 1995.

[20] R. Rojas, *Neural Networks—A Systematic Introduction*, Springer, 1996.